Design and Implementation of Printed Spiral Coils used in Wireless Power Transmission Systems for Implantable Biomedical Devices

Dr. Ahmed S. Ezzulddin
ase.uot@gmail.com
University of Technology – Electrical Engineering Department

Ahmed A. Ibraheem
ahmed.alyasry.gh@gmail.com
University of Technology – Electrical Engineering Department

Abstract: *This paper proposed a small size and efficient square-shaped printed spiral coils (PSCs) at 13.56 MHz to be used for implantable biomedical devices. Detailed modeling of PSCs is presented. A design methodology has been applied to theoretical closed-form equations using MATLAB to optimize the wireless link of a 12×12 mm2 implantable coil example with 10 mm relative distance. All results are validated with the simulation using an electromagnetic field solver HFSS 14.1. Also, the PSCs has been implemented for verification using FR4 printed circuit board. The results show that optimized coil pairs achieved efficiency up to 80% at face to face relative distance of 10 mm in the air.*

Keywords: wireless power transfer, Inductive coupling, Printed spiral coil, Implantable biomedical devices.

1. Introduction

Wireless power transfer (WPT) via inductively coupled coils has triggered a great interest of research, related to its wide collection of applications, such as wireless power transfer to desktop peripheral [1], charging of portable consumer electronics [2, 3], and implanted biomedical devices [4, 5].

The use of a wireless inductive link to transfer power and data to implanted microsystems devices to monitor and stimulate nerves and muscles is raising. The main design interest in the implantable devices field is to reduce the patient discomfort and hazard of infection. Usually, implanted devices are obtaining power using implanted batteries, cause chemical burns and risks. Because of the chemical side effect of the implanted and its limited lifetime, researchers have developed an appropriate substitute method for powering implanted devices using inductively coupled power link. It believed that the inductive link approach is the most favorable technique for implanted devices. Its advantages ensure continuous availability of enough levels of power to the implanted devices. In addition, WPT can be used for a long time and within the patient's activities [6].

Figure 1 is clearly elucidated an equivalent circuit diagram of wireless power transfer WPT link. L_1 and L_2 are the inductance of the primary and secondary PSCs, respectively. L_1 is typically driven by class E amplifier which has need of only a single transistor switch and has the benefit of high efficiency. C_p and R_s are the parasitic capacitance and resistance of PSCs, respectively. C_1 and C_2 are tuning capacitors added to PSCs to make the transmitter and receiver resonate on the same frequency.

In practice, the secondary coil loaded by some electrical loads such as voltage regulator and rectifier. These loads are epitomized by load resistance R_L. The biggest power loss typically happens in the transmitter coil parasitic resistance R_{s1} followed by R_{s2} and the power load condition within R_L on the receiver side. The latter deemed to be more influential because it is surrounded by the tissue [7]. There is also power loss within the external source,

which typically represents an efficient class-E power amplifier. If the operation frequency is chosen below 20 MHz, the power loss within the surrounding tissue can be ignored [8, 9]. A 13.56 MHz ISM band has been chosen which compatible with RFID standards [10]. The overall power transmission efficiency is often dominated by efficiency link η_{link} between transmitter and receiver which that will be focused during the rest of this paper.

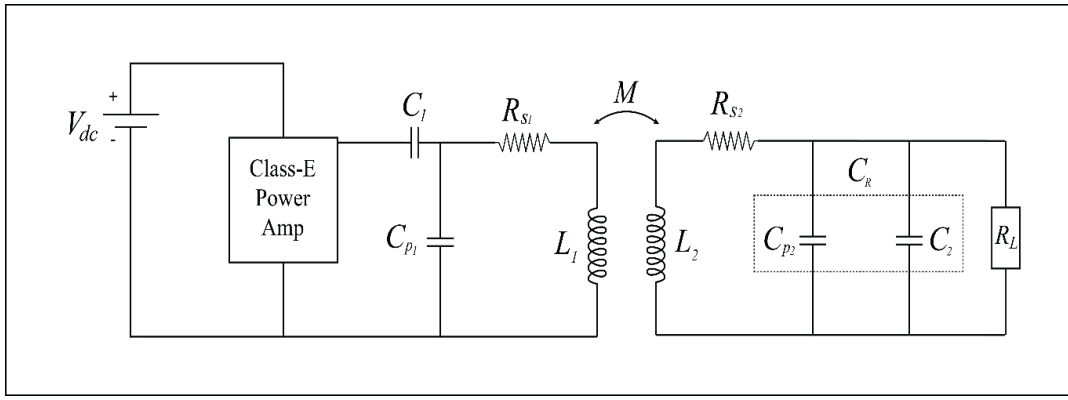

Figure 1: Equivalent circuit diagram of WPT link.

Recently, using a printed spiral coil (PSC) in inductive coupling links has got a considerably of attention. In comparison with wire-wound coils, this type of coils has an advantage from a planar structure which makes them more suitable for implanted systems located underneath the skin or within the epidural space. Furthermore, PSCs can be easily manufactured by standard fabrication technologies.

2. Design of Printed Spiral Coils

In this section, optimal printed spiral coils (PSCs) based on design procedure described in [11]. Design constraints of the application and the fabrication process are listed in Table I. The size of the implanted has been chosen to be 12×12 mm^2. The coupling distance between the PSCs (d_r) is considered 10 mm. The PSCs are designed with 0.25 mm spacing to compatible with

constraints imposed by fabrication technology in Iraq. The final results of the optimized design example are shown in Table II.

Table I: Design constraints imposed by application and fabrication process.

Parameters		Symbol	Design Value
Design constrains	Receiver coil outer diameter	d_{o2}	12 mm
	Distance between coils	d_r	10 mm
	Operating frequency	f	13.56 MHz
	Secondary load resistance	R_L	500 Ω
	Minimum conductor spacing	s_{min}	0.25 mm
	Conductor thickness	t_c	0.07 mm
	Resistivity of material	ρ	16.8 nΩm
	Substrate thickness	t_s	1 mm
	Substrate dielectric constant	ϵ_{rFR4}	4.4

Table II: Optimized PSCs geometries from theoretical design procedure results.

Parameters	TX	RX
d_o (mm)	32	12
d_i (mm)	6.1	5
n (turns)	16	7
w (mm)	0.55	0.25
s (mm)	0.25	0.25

3. Printed Spiral Coils Simulation and Results

To verify the model, Figure 2 shows the model of PSCs constructed in HFSS 14.1 on a distance in the air to find the electromagnetic efficiency. The inductance, resistance, parasitic capacitance, quality factor and coupling coefficient can be calculated from Z-parameter in Figure 3 by using (1)-(5), [12-14]

$$L_1 = \frac{\mathrm{Im}(Z_{11})}{2\pi f}, \quad L_2 = \frac{\mathrm{Im}(Z_{22})}{2\pi f} \tag{1}$$

$$R_{s1} = \mathrm{Re}(Z_{11})(1-4\pi^2 f^2 L_1 C_{p1})^2 \,, \quad R_{s2} = \mathrm{Re}(Z_{22})(1-4\pi^2 f^2 L_2 C_{p2})^2 \tag{2}$$

$$C_{p1} = \frac{1}{4\pi^2 SRF1^2 L_1}, \quad C_{p2} = \frac{1}{4\pi^2 SRF2^2 L_2} \tag{3}$$

$$Q_1 = \frac{\mathrm{Im}(Z_{11})}{\mathrm{Re}(Z_{11})} \,, \quad Q_2 = \frac{\mathrm{Im}(Z_{22})}{\mathrm{Re}(Z_{22})} \tag{4}$$

$$k = \sqrt{\frac{\mathrm{Im}(Z_{12})\mathrm{Im}(Z_{21})}{\mathrm{Im}(Z_{11})\mathrm{Im}(Z_{22})}} \tag{5}$$

At different loading condition, Power transfer efficiency link can be calculated after introduce loaded quality factor Q_L as [15]

$$Q_L = 2\pi f C_R R_L \tag{6}$$

$$\eta_{\mathrm{link}} = \frac{k^2 Q_1 Q_2^2}{(Q_L+Q_2)\left(\frac{Q_2}{Q_L}+k^2 Q_1 Q_2+1\right)} \tag{7}$$

Maximum power transfer efficiency can be determined as

$$\eta_{\max} = \frac{k^2 Q_1 Q_2}{\left(1+\sqrt{1+k^2 Q_1 Q_2}\right)^2} \tag{8}$$

To compute maximum power transmission efficiency, equation (8) was chosen. The simulations of the WPT link were achieved at different transmission distances. In all these case, the inductance and resistance almost remain unchanged, but the mutual coupling was affected directly by this change. The Inductance and quality factor of the PSCs is plotted in Figure 4. The coupling coefficient k of the model can suitably be predicated when (5) is applied as shown in Figure 5. Maximum efficiency of WPT link at different operating frequencies shown in Figure 6. The simulation tests were done for 10 mm transmission distance. The proposed WPT link can determine the maximum efficiency of the power transmission in the entire range of operating frequencies. The result can clearly identify the power transmission efficiency value at desired operation frequency also illustrated the optimal operating frequency at which the power transmission efficiency reaches its peak value at 25 MHz. The designer may prefer to operate nearby this frequency to capture a maximum amount of power by the

receiver, where the power efficiency is the most important requirement of the system.

Figure 7 compares the maximum power transmission efficiency (η_{max}) at different relative distances whereas the operation frequency fixed at 13.56 MHz. The results show that the calculated and simulated values are in agreement. In the next step of simulation has been accomplished to capture the effect of load resistance on the power transmission efficiency (η_{link}). The load resistance was varied while the transmission distances and operation frequency was kept at 10 mm and at 13.56 MHz, respectively. Figure 8 verifies that η_{link} reach toward η_{max} at an optimal load resistance of 500 Ω. Again the proposed model has given the simulation results in an agreeable manner. Employing this model, designers can realize the optimal operating condition and design the best efficient WPT system. Table III shows the final geometries and parameters results of the applied WPT link.

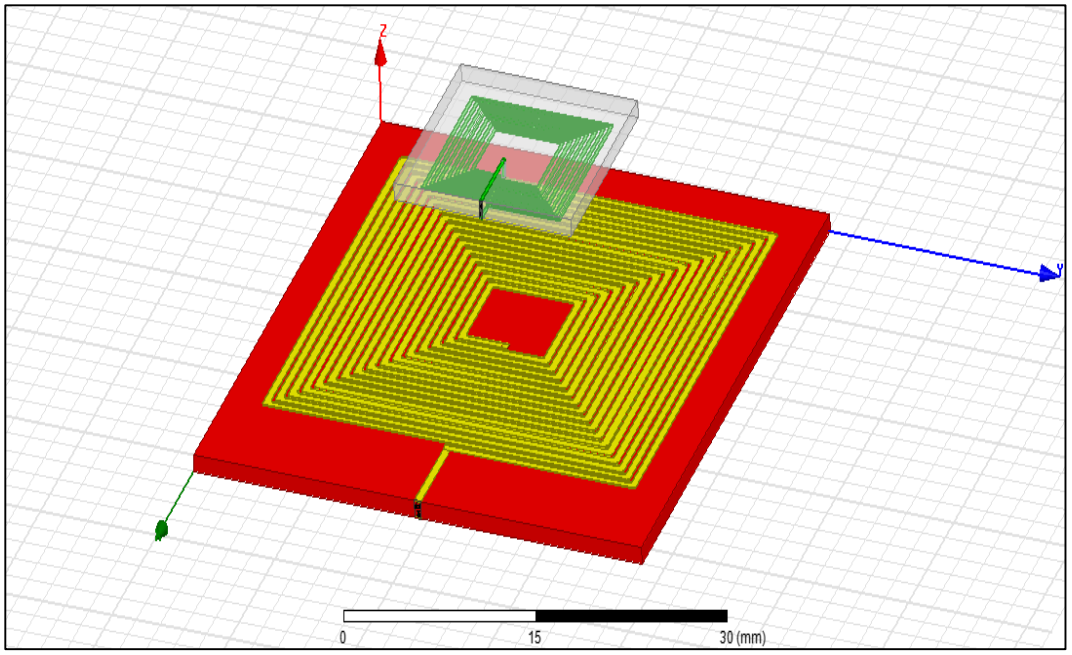

Figure 2: 3D PSC model constructed in the electromagnetic field solver HFSS 14.1 simulator.

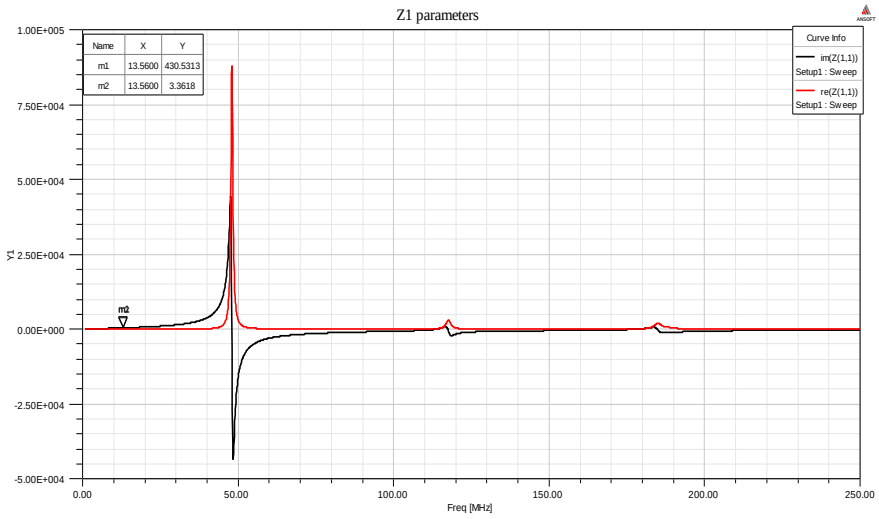

(a)

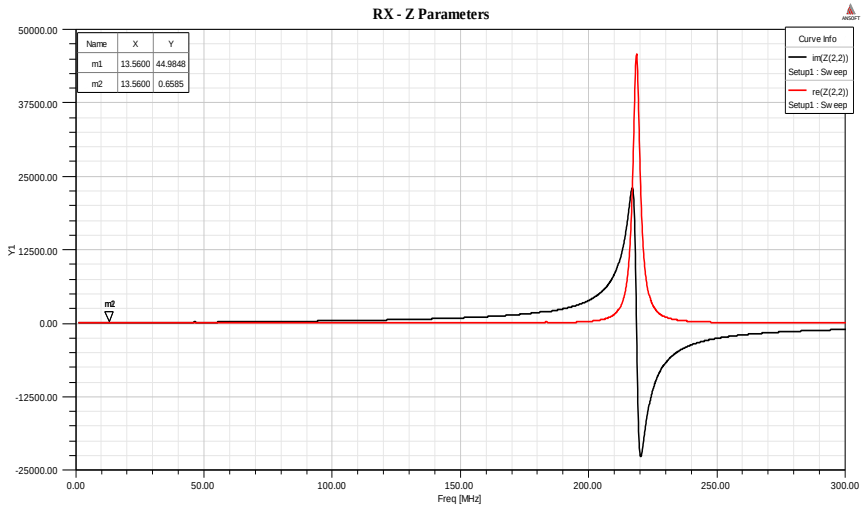

(b)

Figure 3: Real and imaginary part represents the modeling of the PSCs for (a) Transmitter and (b) Receiver.

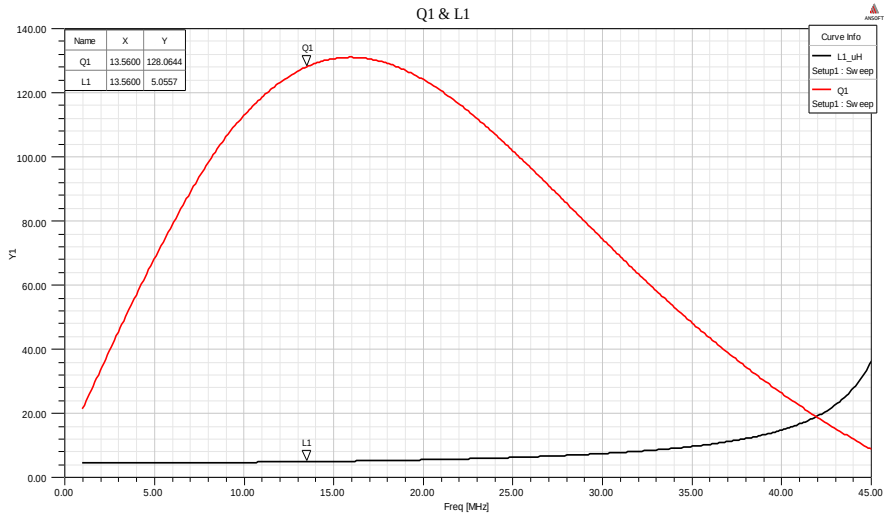

(a)

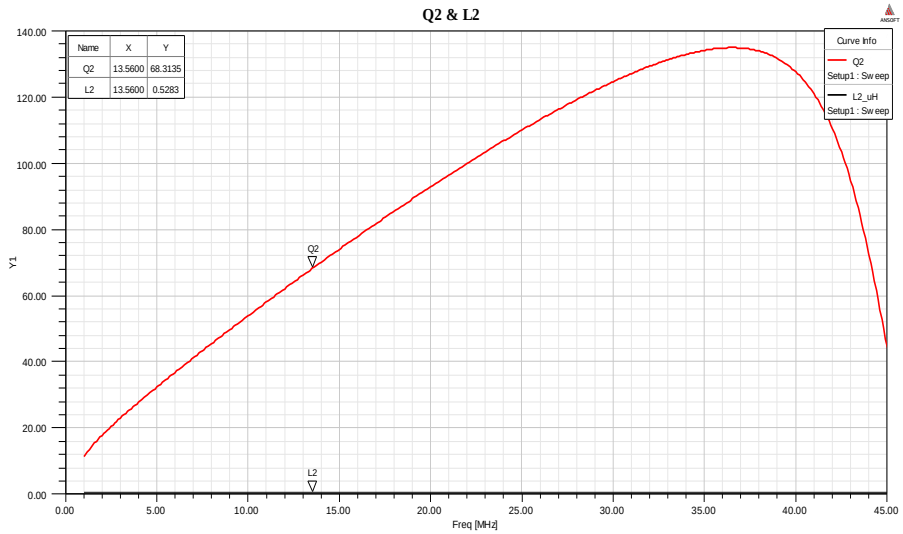

(b)

Figure 4: Simulated *L* and *Q* of PSCs for (a) Transmitter and (b) Receiver

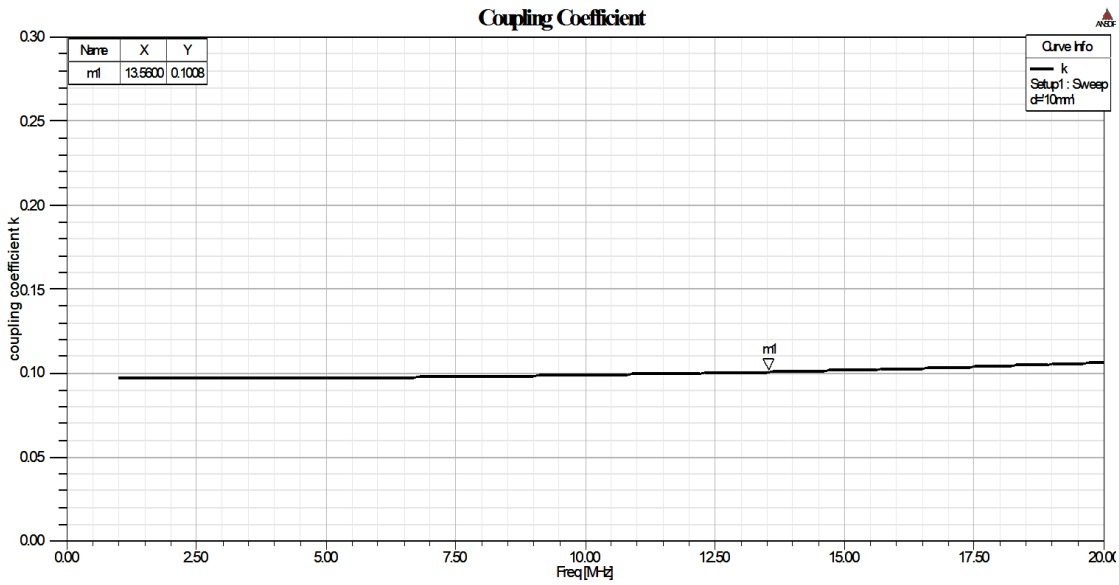

Figure 5: Predicted coupling coefficient k at 10 mm distance.

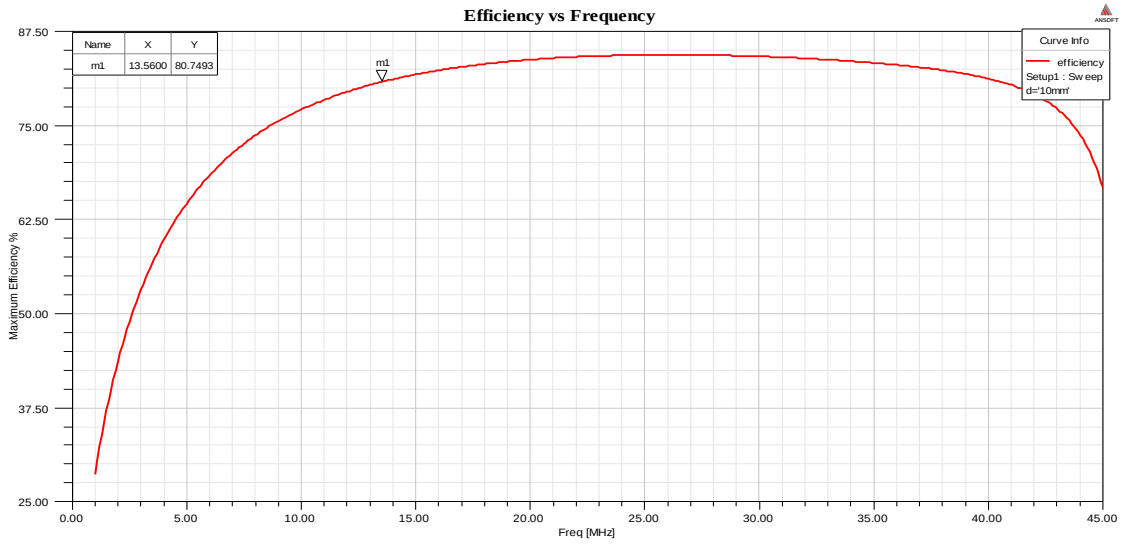

Figure 6: Maximum power transmission efficiency at 10 mm distance for different operating frequencies.

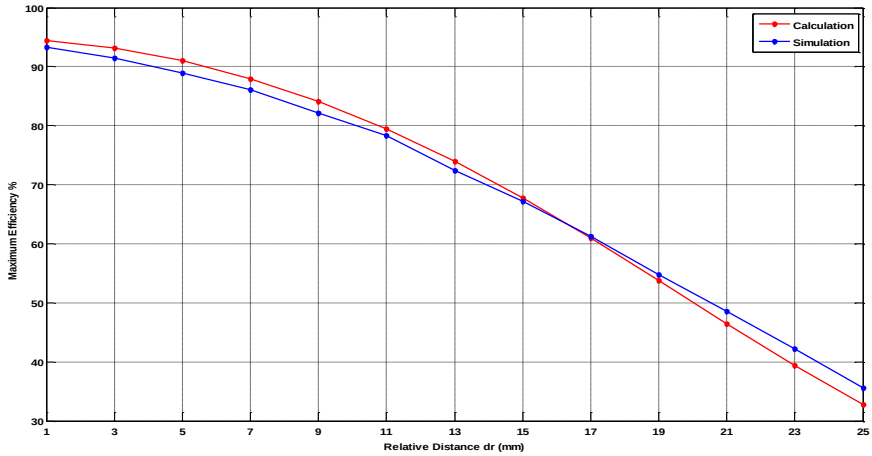

Figure 7: Calculated and simulated maximum power efficiency at different transmission distance with 13.56 MHz operating frequency.

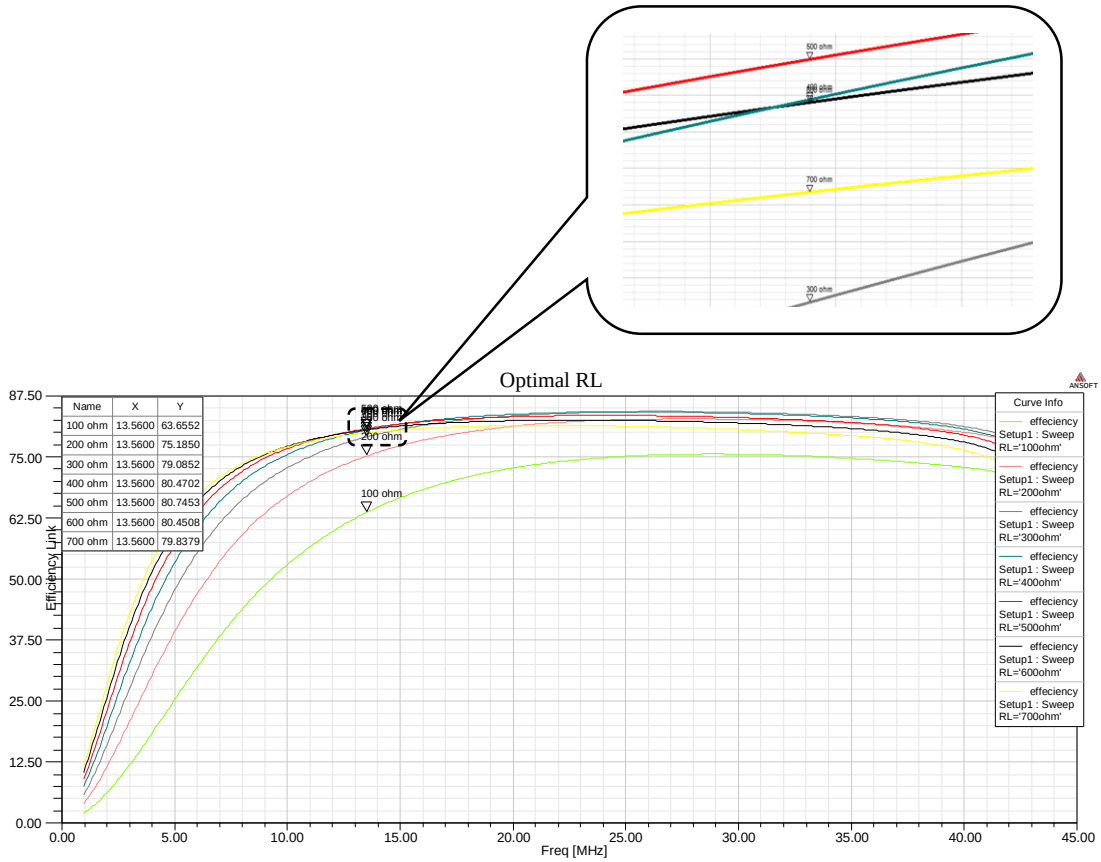

Figure 8: Efficiency of the link at different load resistance at 13.56 MHz Operating frequency and 10 mm transmission distance.

4. Printed Spiral Coils Implementation and Experimental Results

The proposed transmitter and receiver PSCs has been fabricated on 1 mm FR4 substrate and characterized them to more validate our PSC design technique. Figure 9 shows the transmitter and receiver PSCs are designed using ADS 2014 software and then converted to Gerber file which agrees with printer machine software. The two PSCs after fabrication are shown in Figure 10

and Figure 11. Figure 12 shows the PSCs measurement setup was mounted using a plastic bracket, aligned, and held in parallel at desired coupling distance. MS4642A vector network analyzer (VNA) has been used to measure the Z-parameters of coupled PSCs pair. Z-parameters are used to calculate k, Q_1 and Q_2 as we have already shown which was then substituted in (2.29) to find the maximum power transmission efficiency. The results are illustrated from Figure 13 to Figure 16 which was not very satisfactory compared with theoretical and simulation results.

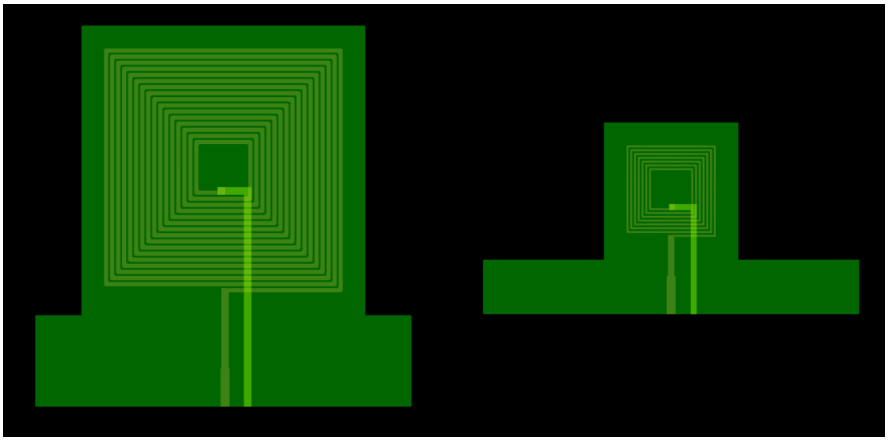

Figure 9: Transmitter and receiver PSCs design on ADS software.

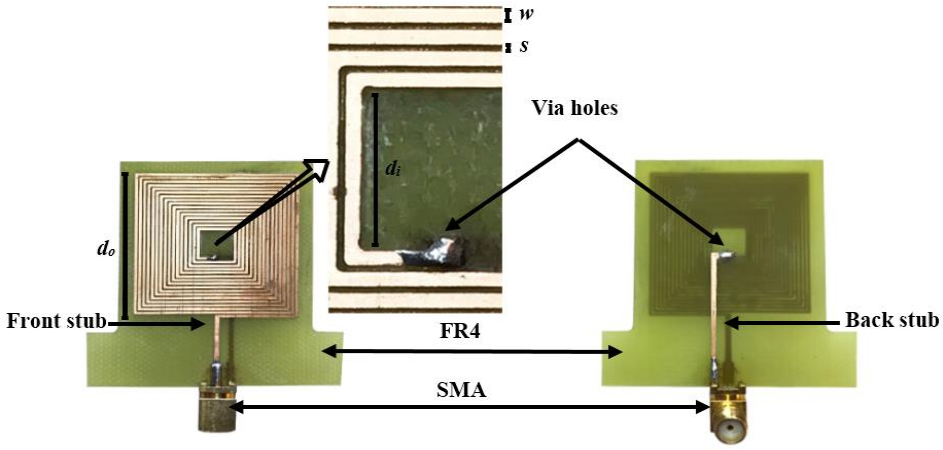

(a) **(b)**

Figure 10: Photograph of the PSC transmitter (a) front view (b) back view.

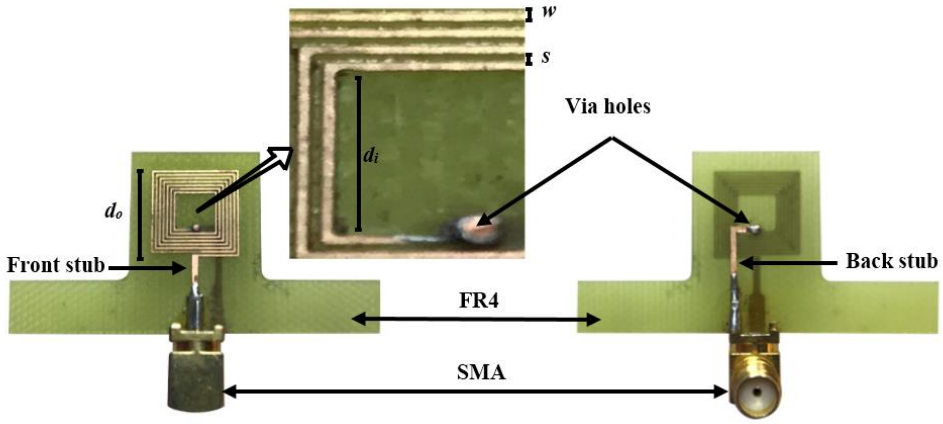

(a) **(b)**

Figure 11: Photograph of the PSC receiver (a) front view (b) back view.

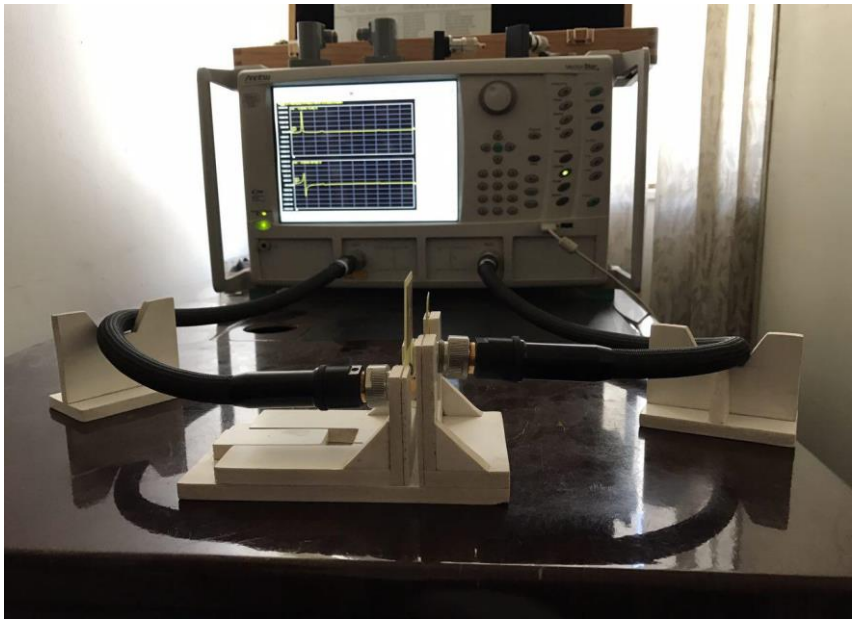

Figure 12: Transmitter and receiver PSCs under test.

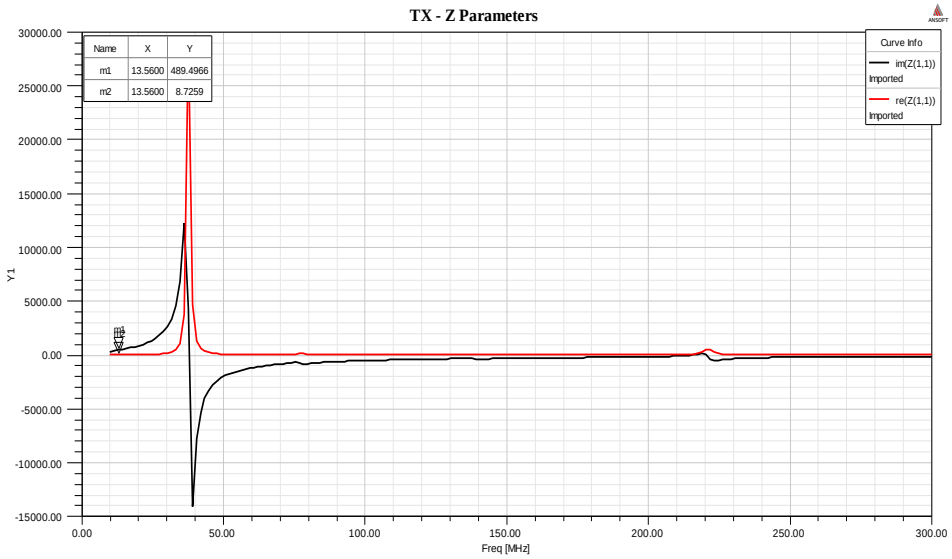

(a)

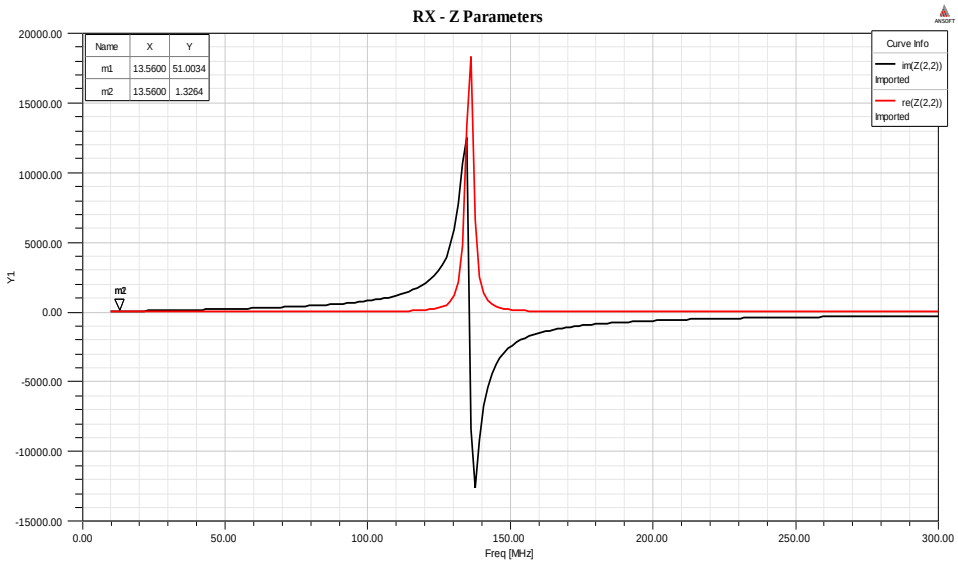

(b)

Figure 13: Measured real and imaginary part represents the modeling of the PSCs (a) transmitter and (b) receiver.

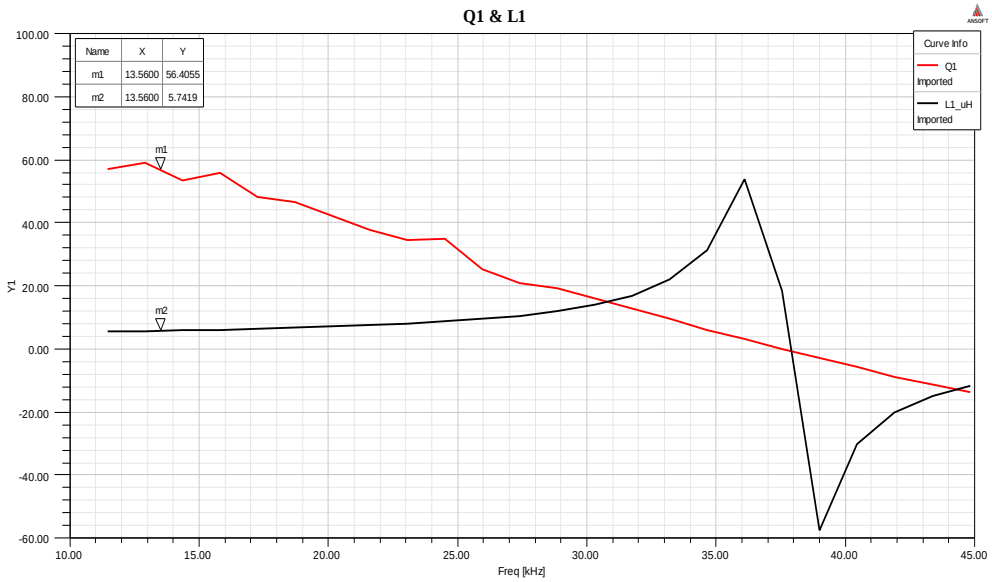

(a)

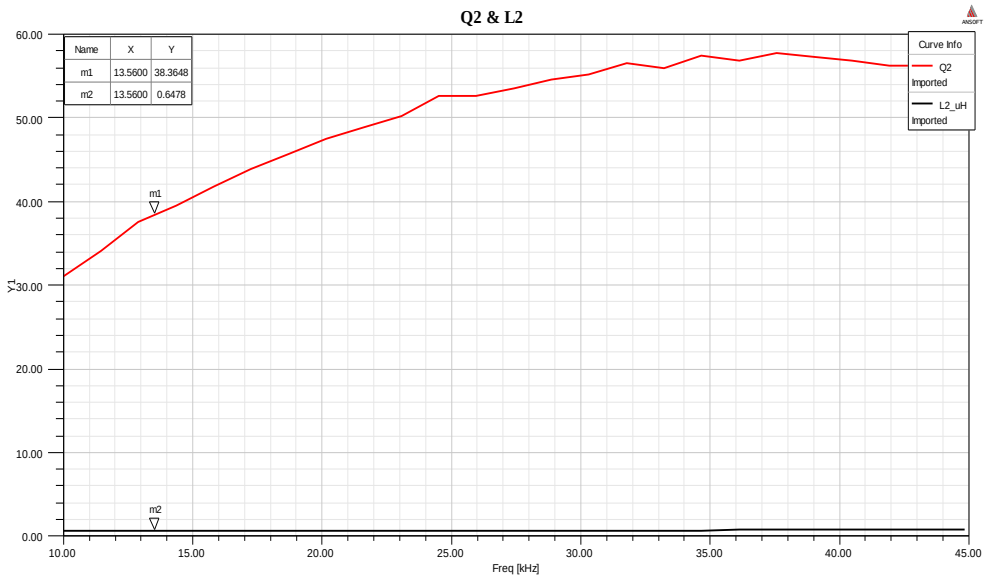

(b)

Figure 14: Measured L and Q of PSCs for (a) transmitter and (b) receiver.

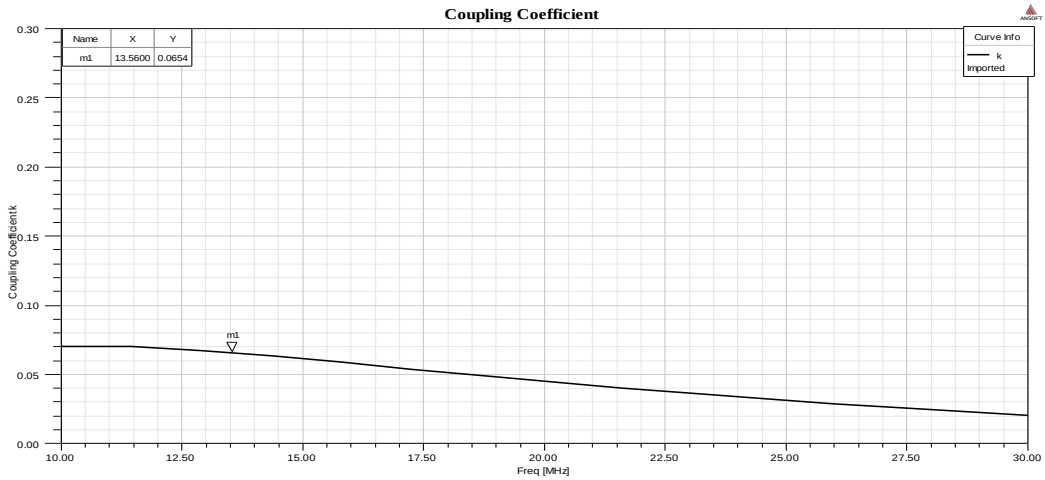

Figure 15: Measured k of the PSCs pair at 10 mm distance.

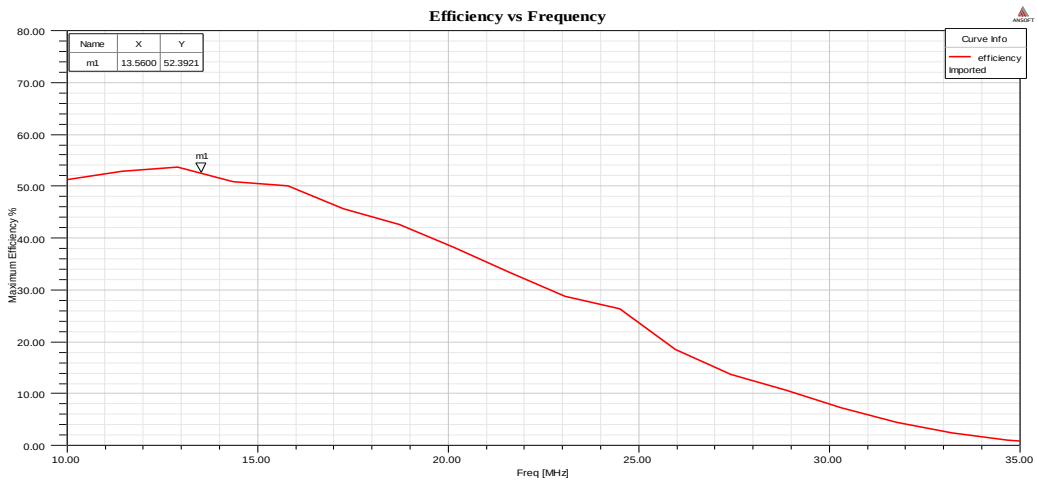

Figure 16: Maximum power transmission efficiency at 10 mm distance for a different operating frequency.

The Z-Parameters in Figure 19 show that there is an additional increment in measured resistances were more lossy than simulation results and increased resistance values. This result in degrading the quality factors of the coils as shown in Figure 20. The reason was presumably due to:

1- The quality and purity of the FR4 substrate used,
2- The conductivity of the copper traces is less than perfect value,
3- Welding points of vias and SMA connectors and their effect on the overall series resistance of the transmitter and receiver PSCs, and
4- The reflected impedance mismatch of coil impedance.

Table III: Optimized PSC pair geometries and inductive link parameters from simulation and measurement results¤.

Parameters	TX		RX	
	Simulation	Measurement	Simulation	Measurement
d_o (mm)	32		12	
d_i (mm)	6.1		5	
n (turns)	16		7	
w (mm)	0.55		0.25	
s (mm)	0.25		0.25	
L (µH)	5.05	5.74	0.528	0.648
R_s (Ω)	3.07	6.75	0.653	1.3
C_p (pF)	2.27	3.056	1	2.145
C_1/C_2(pF)	25	21	260	210
Q	128	56.40	68	38.36
SRF (MHz)	47	38	218	135
k_{cal}♦	0.1041			
k_{sim}•	0.1008			
k_{meas}*	0.0571			
η_{link_cal}♦	79.99%			
η_{link_sim}•	80.74%			
η_{link_meas}*	51.65%			

¤For perfectly aligned PSCs with a nominal coupling distance of 10 mm at 13.56 MHz and 500 Ω load.
♦Calculation results, •Simulation results, and *Measurement results.

The reasons mentioned above also have a direct effect on the coupling coefficient k due to drop in mutual coupling M. Additionally, k is affected by any error in alignment and distance that fades the desired position, also the material of bracket and extra parts in FR4 degrade the signal. Table III illustrates final PSCs geometries and inductive link parameters from simulation and measured results comparison.

5. Conclusion

Optimal printed spiral coil pair used in wireless power transfer system for implantable biomedical devices is presented in this paper. We have devised a simple design procedure for optimizing the gross geometry of printed spiral coils to achieve maximum power transmission efficiency. Numerical calculation results and HFSS electromagnetic simulation denote that the power transmission efficiency of WPT link in air medium are in agreement and reached 80%, which validates the concept of the physical models. Experimental results offered efficiency lower than simulation results which degrade from 80.78% to 51.65%. The degradation in results is due to the accuracy and quality of the manufacturing technology used.

References

[1] Meyer P., Germano P., Markovic M., and Perriard Y., "Design of a contactless energy-transfer system for desktop peripherals," IEEE Transactions on Industry Applications, vol. 47, no. 4, pp. 1643-1651 Jul./Aug. 2011.

[2] Waffenschmidt E., "Wireless power for mobile devices," IEEE International Telecommunications Energy Conference, Amsterdam, Oct. 2011.

[3] Marques H., and Borges B., "Contactless battery charger with high relative separation distance and improved

efficiency," International Telecommunications Energy Conference, Oct. 2011.

[4] Jow U., and Ghovanloo M., "Design and optimization of printed spiral coils for efficient transcutaneous inductive power transmission," IEEE Transactions on biomedical circuits and systems, vol. 1, no. 3, pp. 193-202, Sep. 2007.

[5] Yang C., Chang C., Lee S., Chang S., and Chiou L., "Efficient four coil wireless power transfer for deep brain stimulation," IEEE Transactions on Microwave Theory and Techniques, pp. 1-12, 2017.

[6] Ashraf M., and Masoumi N., "A fully-integrated power supply design for wireless implantable biosensors," Electrical Engineering (ICEE), 2014 22nd Iranian Conference. IEEE, 2014.

[7] Lazzi G., "Thermal effects of bioimplants," IEEE Engineering in Medicine and Biology Magazine, vol. 24, no. 5, pp. 75-81, 2005.

[8] Vaillancourt P., Djemouai A., Harvey J. F., and Sawan M., "EM radiation behavior upon biological tissues in a radio-frequency power transfer link for a cortical visual implant," Proceedings of 19th Annual International Conference of the IEEE, vol. 6, pp. 2499-2502, Oct. 1997.

[9] Stocklin S., Volk T., Yousaf A., Albesa J. and Reindl L., "Efficient inductive powering of brain implanted sensors," Sensors Applications Symposium (SAS), IEEE, 2015.

[10] Finkenzeller K., RFID Handbook: Fundamentals and Applications in Contactless Smart Cards, Radio Frequency Identification and Near-Field Communication, John Wiley and Sons, 2010.

[11] Ezzulddin, A. S., and Ibraheem, A. A. "Design and Optimization of Printed Spiral Coils used in Wireless Power Transmission Systems for Powering 10 mm2 Receiver Size

at 13.56 MHz Operating Frequency" International Journal of Current Engineering and Technology, Vol.7, No.5, Sept./Oct. 2017.

[12] Yang Z., Liu W., and Basham E., "Inductor modeling in wireless links for implantable electronics," IEEE Transactions on Magnetics, vol. 43, no. 10, pp. 3851-3860, Oct. 2007.

[13] Wu W. and Fang Q., "Design and simulation of printed spiral coil used in wireless power transmission systems for implant medical devices," Engineering in Medicine and Biology Society, EMBC, 2011 Annual International Conference of the IEEE, pp. 4018-4021, 2011.

[14] Mehri S., Ammari A. C., Ben J., Slama H., and Rmili H., "Geometry optimization approaches of inductively coupled printed spiral coils for remote powering of implantable biomedical sensors," in Proceedings of the Global Summit on Computer and Information Technology (GSCIT ’14), pp. 1-11, Sousse, Tunisia, June 2016.

[15] Raju S., Parawoto C. C., Chan M., and Yue C. P., "Modeling of on-chip wireless power transmission system," 2015 IEEE International Wireless Symposium (IWS), IEEE, 2015.

التصميم والتنفيذ للفائف اللولبية المطبوعة المستخدمة في أنظمة نقل الطاقة اللاسلكية للأجهزة الحيوية المزروعة

د. أحمد سعدون عز الدين
ase.uot@gmail.com
الجامعة التكنولوجية – قسم الهندسة الكهربائية
أحمد عيّاد إبراهيم
ahmed.alyasry.gh@gmail.com
الجامعة التكنولوجية – قسم الهندسة الكهربائية

المستخلص

هذا البحث قدم زوج من اللفائف المربعة المطبوعة ذات حجم صغير تعمل على تردد 13.56 MHz لأجل استخدامها في الاجهزة الطبية القابلة للزرع. نمذجة مفصلة للفائف المطبوعة قد تم عرضها. طبقت منهجية تصميم معتمدة على معادلات نظرية مثبتة بأستخدام MATLAB لتحسين الوصلة اللاسلكية بحجم لفائف مزروعة 12×12 mm وعلى مسافة 10 mm. جميع النتائج أُثبتت بأستخدام برنامج المحاكاة HFSS 14.1 وكذالك نُفذت عملياً بأستخدام الواح FR4. وأظهرت النتائج أن أزواج اللفائف المثلى قد حققت كفاءة تصل الى 80% وجهاً لوجه وعلى مسافة 10 mm في الهواء.

الكلمات الرئيسية: أنظمة نقل الطاقة اللاسلكية، الاقران الحثي، اللفائف اللولبية المطبوعة، الأجهزة الطبية المزروعة.